Smart Structures and Systems, *Vol. 28, No. 3 (2021) 375-390*
https://doi.org/10.12989/sss.2021.28.3.375

Combination of an inverse solution and an ANN for damage identification on high-rise buildings

Quy T. Nguyen*[1,2] and Ramazan Livaoğlu [1a]

[1] *Civil Engineering Department, Bursa Uludağ University, 16059 Nilüfer/Bursa, Turkey*
[2] *Department of Mechanics of Structures, Ho Chi Minh City University of Transport, Ho Chi Minh City, Vietnam*

(*Received November 25, 2020, Revised May 25, 2021, Accepted May 26, 2021*)

Abstract. Structural health monitoring (SHM) is currently applied to control regularly the health of high-rise buildings which have deteriorated after being subjected to a sudden loading. Damage detection at element levels of a structure consisting of an enormous number of elements becomes the main objective. In this study, the complicated problem is simplified by a two-step solution. Damaged storeys are preliminarily detected before a full damage scenario at an element level is achieved. In Step 1, to overcome the issues related to the huge number of degrees of freedom (DOFs), the full building is simplified to a beam-like system using the Guyan condensation technique. As the natural characteristics of the two lowest modes at the intact and a damaged stage are obtained, the eigenvalue problem based inverse solution is applied to approximately detect damaged storeys. Furthermore, an updating procedure that is proposed in this study effectively enhances the first prediction. In Step 2, an artificial neural network (ANN) model is designed to indicate damaged members on detected storeys using only the first three modal modes. Compared to other approaches applied to detect damages on high-rise buildings, the robustness of the proposed method is that the required number of lowest modal modes is two and three in Step 1 and Step 2 respectively. Furthermore, regardless of the extension of the building in the horizontal direction, only one lateral displacement of each storey is measured to detect damaged storeys in Step 1 and generally detect damaged elements in Step 2. For light and asymmetrical damage scenarios, two more vertical displacements should be considered to obtain accurate element-level detection. However, for all cases, the required number of DOFs is significantly lower than the full system.

Keywords: artificial neural network ANN; damage detection; damage localization; high-rise buildings; structural health monitoring

1. Introduction

SHM is divided into four levels: damage presence indication, its localization, severity estimation, and a prediction of the remaining service life of structures according to Rytter (1993). The first three levels are in the broader category of damage assessment according to Kim and Stubbs (2002) and Yan *et al*. (2007). Tran-Ngoc *et al*. (2020) stated that SHM based on non-destructive methods has been the most popular approach. The changes in the modal data of a system are used to detect damages on it. Natural frequency shifts are considered as sensitive damage indicators of structural integrity according to Cerri and Vestroni (2000) and Hamad *et al*. (2011). Yan *et al*. (2007) pointed out that the measurement of natural frequency cannot provide enough information for structural damage detection, especially for damage localization. Moreover, this modal parameter is influenced by the environmental conditions as stated by Gillich *et al*. (2019) and Tran-Ngoc *et al*. (2018). Rizos *et al*. (1990) used the changes in mode shapes to find the crack location and estimate the depth but the accuracy progressively gets smaller with more complicated structures. Another modal information, modal strain energy (MSE) also took interest from Ndambi *et al*. (2002), Wahalthantri *et al*. (2012), and Khatir *et al*. (2019). However, the issues related to small damages and the number of required mode shapes were witnessed. Kim and Stubbs (1995a, b, 2002) established MSE based damage indices (DIs) using only a few available modes. The method was successfully verified on larger structures such as steel portal frames, steel frames with braces, offshore jacket platforms. However, the approach requires a huge number of measurement points. Particularly, the vibration information at each node is required.

The aforementioned approaches may not be suitable for damage identification in huge structural systems such as high-rise buildings because of the complexity as well as the limited number of measured DOFs in practice. Dinh-Cong *et al*. (2019) proposed a practical method for damage identification using the Lightning Attachment Procedure Optimization (LAPO) algorithm and model reduction. The full mechanical matrices of the building were reduced effectively using an iterated improved reduction system (IIRS) technique. The method successfully identified damage on a 2-dimensional (2D) 4-story 3-bay steel frame. In the Finite Element (FE) model, there are a total of 16 vibration nodes making 48 DOFs. However, only 10 biaxial

*Corresponding author, Ph.D. Student,
E-mail: nguyenthuequy@gmail.com
[a] Professor, E-mail: rliva@uludag.edu.tr

ISSN: 1738-1584 (Print), 1738-1991 (Online)

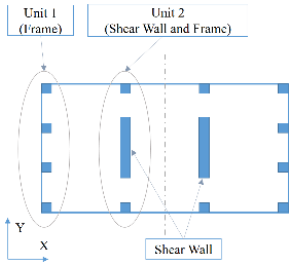

(a) Plan of 3D building

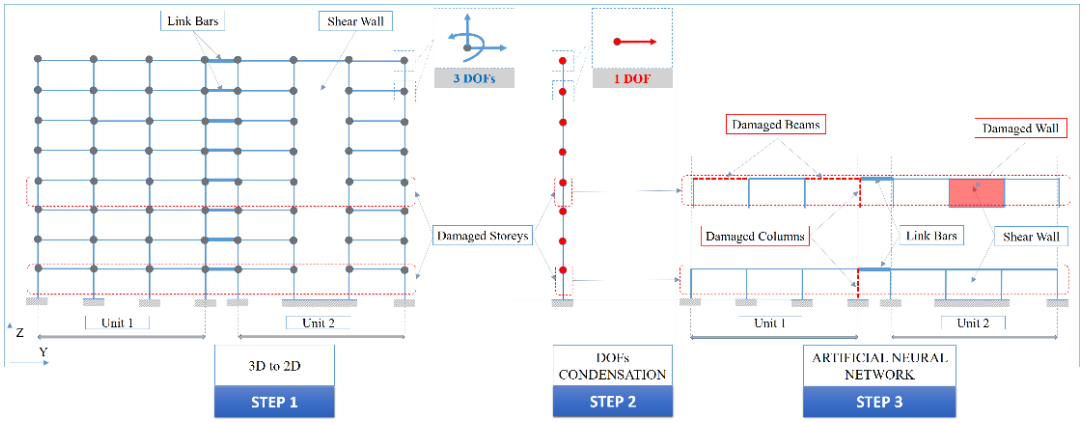

(b) Three-step procedure

Fig. 1 Damage identification procedure

sensors are mounted on the perimeter of the structure. The sensor network is to collect 20 translational DOFs, about 41.7% of the total DOFs. For high-rise buildings, this ratio seems not to be reasonable. On the other hand, ANN approaches are considered effective to detect damage on large structures. ANN is a fast and accurate tool for solving complex problems in the field of engineering, science, and manufacturing according to Khatir *et al*. (2020). Single and double damage cases on a 9-storey shear frame were successfully obtained using an ANN model proposed by Paral *et al*. (2019). Nguyen *et al*. (2020) successfully combined the use of transmissibility functions with ANN to assess damage in Nam O bridge in Vietnam, a truss bridge. Chang *et al*. (2018) successfully detected damage on a 3-D building, especially a scaled twin tower using an ANN based method. Similar to Dinh-Cong *et al*. (2019), the full structure is firstly simplified to a beam-like system but using a different approach, a stochastic system identification technique. The outstanding of this study is that the number of sensors is equal to the number of stories. The slabs are considered as some lumped masses on the simplified system. Although the proposed approach was verified successfully, four issues should be taken into account. First, the study focused only on story-level detection. Second, the rotation of the slabs on high-rise buildings might be not considered adequately, especially on the upper parts. Therefore, a simplified system without considering rotational DOFs may not be adequate to represent a high-rise building. Third, the proposed ANN was trained using seven bending mode shapes to detect damages on a 7-lumped mass system. It is true that for high-rise buildings, such information for all bending modes, especially high modes, may not be obtained easily with high accuracy in practice. Finally, only for a 7-floor building, a total of 279936 (6^7) combinations was used to build the input data for the ANN model. It may be a big challenge to apply the method to high-rise buildings.

It is true that ANN approaches are effective but applying directly ANN based methods to high-rise buildings is a costly computation process. In this study, damaged storeys are detected preliminarily. Thereafter, the ANN method is applied only on the determined damaged storeys to detect damaged elements. That significantly lowers the number of variables in the ANN model. Besides that, to overcome the issue in building the combinations of the ANN model, Bakhary (2008) applied the orthogonal array (OA) method that was introduced by Hedayat *et al*. (1999) to build the first combination set considering only two cases, damaged and undamaged. The approach reduces effectively the number of combinations from 2^{NF} to 2xNF (NF is the number of factors or unknown variables). After that, for each combination in the first set, a wide range of damage severity is distributed to the damaged members using the Latin hypercube sampling technique. According to Helton and Davis (2003), the technique is employed to ensure that the training data is generated uniformly over each area within the determined range of damage severities. This approach is applied to build the input data of the ANN model in this study.

High-rise buildings are generally comprised of columns, beams, slabs, and shear walls. Detecting damage on full structures is impossible because of the huge number of DOFs. A step-by-step procedure as seen in Fig. 1 is introduced for damage identification on high-rise buildings.

It is divided into three steps. The first one is idealizing a three-dimensional (3D) building to a two-dimensional (2D) frame. After that, an eigenvalue problem based updating method is applied to detect damaged storeys. Finally, an artificial neural network is trained to localize damage and estimate damage severity on preliminarily detected storeys.

For Step 1, according to Smith and Coull (1991), on each storey, the lateral displacement of the slab represents the lateral deflections of columns and shear walls. Based on that one of the most commonly used methods can be seen through the example in Fig. 1. The typical plan of the 3D frame shows that the frame contains columns, slabs, and shear walls. The lateral response of the structure belong to the Y-direction is considered herein as an example. Approximately, according to ACI Committee Report SP-97 (1985), the lateral resistance in the Y-direction is contributed by the four 2D frames. The structure has a symmetrical plan so only Unit 1 and Unit 2 are considered then. The combination of them can be displayed as the idealized 2D frame. In the idealized model, the connection between units is approximately defined as link bars that have a significantly high rigid compared to other bending elements such as columns and beams. For the shear walls, some idealized models are used to define the response of shear walls. The behavior of walls can be simplified as the response of frame elements such as wide columns and braced frames. As a result, the simplified frame is possibly analyzed by using only frame elements.

For Step 2, damaged storeys are indicated first using an eigenvalue problem based method that is the main object of another article written by the authors of this study (Nguyen 2020). The main idea of the method is that all 3 DOFs (translational and rotational) at each node on each storey are condensed into only lateral DOF as seen in Fig. 1(b). The mechanical model is rapidly determined then. The eigenvalue based inverse solution is rapidly implemented to detect damaged storeys using the lowest modes that are obtained by a sensor network in which only one lateral displacement per floor is required. Thereafter, an updating procedure is proposed to enhance the first prediction to a higher level of accuracy.

The method has been validated numerically on a 30 storey-4 bay building and experimentally on a 3 storey steel frame in the original work. Through the validations, the robustness of the updating procedure is confirmed as there is no error witnessed for storey-level detection. In the numerical investigation, the damage severity of detected storeys was predicted precisely while a slight error of about 12% was witnessed in the empirical validation. In this study, the main idea of the updating approach is briefly repeated, and extended observation of different damage scenarios, especially light categories that have not been mentioned before is introduced. Element-level detection is also the second objective of this study.

For Step 3, after detecting damaged floors, an ANN model is designed to locate damaged columns and beams. The network mainly requires two modal information from each storey, one horizontal displacement, and the floor rotation. The first information is reused from the updating procedure. The latter can be approximately stood for by the ratio between the two vertical displacements at the starting point and ending point of each floor. The proposed ANN model is successfully validated on a 20 storey building that has 180 structural members. The first information gives accurate damage locations as a symmetrical damage configure is considered. On the other hand, more complicated modal information is required to achieve a precise damage prediction for an asymmetric damage scenario. A complete damage identification procedure is successfully validated and becomes a promising technique to be considered for a practical application.

The main objective of this study is to introduce damage detection of a building. Therefore, only Step 2 and Step 3 are considered herein. The performance of the proposed method is investigated using numerical simulations only because the approaches have been identified as powerful tools used in many engineering applications according to Khatir and Abdel-Wahab (2019). Besides that, the proposed method is only validated on 2D systems that contain only frame elements such as columns and beams for the purpose of simplification. It is assumed that a model simplification contains some inevitable errors. However, those issues are expected not to significantly affect the damage detection results. This manuscript illustrates inevitable errors caused by some approximations during simplifying a 2D system to a beam-like system as well as the computation process. Those errors are also expected to be faced when simplifying a 3D model. Therefore, the numerical validation on a 2D model is assumed to be suitable to focus on the proposed technique for the purpose of simplification. In fact, selecting a 2D problem to validate a new method is also seen in published articles, Yun and Bahng (2000) and Yun *et al*. (2001) with 10-storey 2-bay and frame structure, Dinh-Cong *et al*. (2019) with a 4-story 3-bay frame, Mirzabeigy (2019) with 7-storey single-span frame, and Paral *et al*. (2019) with a 9-story single-span frame.

2. Backbone idea of the eigenvalue problem based updating method

As a structure is under monitored, an eigenvalue problem based inverse solution theoretically can be activated to figure out the health of the system. The solution requires firstly the mechanical properties (stiffness and mass matrices) and the natural characteristics at the healthy state. Then the modal information of a current stage must be measured exactly in field. The input data gives information about the current stiffness matrix. However, the number of DOFs that can be measured in practice is significantly less than the full system. That makes the inverse solution for a full problem impossible. To deal with the incomplete measured modal vectors, vibration mode expansion becomes necessary. However, the measurement errors possibly mix with the errors caused by the vibration mode expansion according to Yan *et al*. (2007). Moreover, using the manner makes the inverse solution extremely big. Alternatively, to activate the eigenvalue problem based inverse solution, the size of the complete stiffness matrix and mass matrix should be reduced appropriately to meet

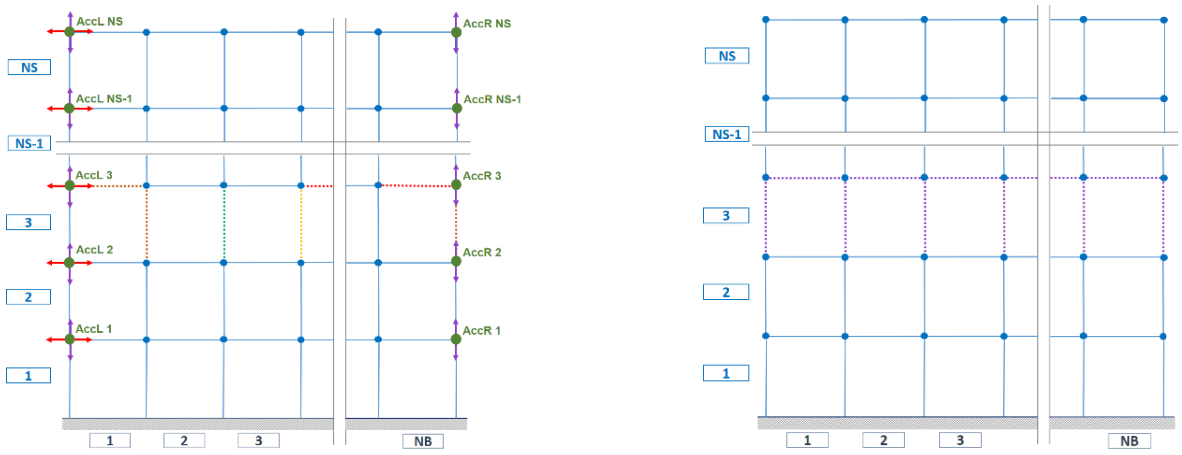

(a) Actual damage scenario (b) Simplified damage scenario

Fig. 2 An approximation

the size of measured data.

Let take the system working in a two-dimensional coordinate (see Fig. 2(a)) as an example. There are NS stories and *NB* bays. Even for the simplest case in which each structural member is considered as one element, the number of DOFs is enormous. The Young's modulus value of each element, *E*, is representative of its health while other parameters such as its cross-section dimension are kept unchanged. In other words, there are total *NE E*-values identical to the number of all elements. However, the complicated problem can be simplified by approximately transferring the actual damage scenario (see Fig. 2(a)) to a simplified damage scenario as Fig. 2(b) in which all of the structural elements on each floor are assigned only one damage severity. The dotted lines in Fig. 2 stand for damage elements and the different colors represent various damage severities. As a storey is damaged, the value of *E* is decreased by the same amount. Consequently, instead of *NE* elements, only *NS* values of *E* are considered. To determine the *NS* values of *E*, the behavior at the starting point and ending point of each storey must be considered. Recognize that at lower modes, all nodes on a similar floor approximately vibrate with the same horizontal amplitude. A simple network of sensors or accelerometers (AccL) displayed in Fig. 2(a) satisfies this purpose. It is noted that AccL and AccR stand for the accelerometers locating on the left and right sides of the structure, respectively. For this configuration, the information about vertical and rotational DOFs is currently ignored from the measurement. The size of the measured eigenvector for each mode now is significantly reduced to *NS* by 1. To activate the eigenvalue problem based inverse solution, the size of the complete stiffness matrix and mass matrix in the intact state should be correspondingly reduced to *NS* by *NS* to fit with the measured eigenvectors. Guyan static condensation procedure appears as an effective solution as all of the DOFs at each storey are condensed into only one lateral DOF.

2.1 Guyan condensation for eigen-problems

The general eigenproblem of a full system with the stiffness matrix, $\boldsymbol{K}$, and the mass matrix $\boldsymbol{M}$ is given as Eq. (1) in which $\boldsymbol{\lambda}$ and $\boldsymbol{\Phi}$ are the eigenvalue (square of frequency) and the corresponding eigenvector (mode shape) of the full model, respectively. Once the DOFs that are kept (master DOFs) and the ones that are condensed (slave DOFs) are determined, the matrices can be rearranged, and consequently, Eq. (1) may be rewritten in a partitioned form as Eq. (2). It is noted that the subscripts *m* and *s* indicate the parameters corresponding to the masters and slaves.

$$(K - \lambda M)\Phi = 0 \tag{1}$$

$$\left(\begin{bmatrix} K_{mm} & K_{ms} \\ K_{sm} & K_{ss} \end{bmatrix} - \lambda \begin{bmatrix} M_{mm} & M_{ms} \\ M_{sm} & M_{ss} \end{bmatrix}\right) \begin{Bmatrix} \Phi_m \\ \Phi_s \end{Bmatrix} = \begin{Bmatrix} 0 \\ 0 \end{Bmatrix} \tag{2}$$

After that $\boldsymbol{K_G}$ and $\boldsymbol{M_G}$ are the reduced stiffness and mass matrices and the eigenvalue problem for an incomplete problem is defined in Eqs. (3)-(5). Let the reduced matrices $\boldsymbol{K}_G$ and $\boldsymbol{M}_G$ be divided into two parts, the first parts include $\boldsymbol{K}_f$ equal to $\boldsymbol{K}_{mm}$ and $\boldsymbol{M}_f$ equal to $\boldsymbol{M}_{mm}$ while the remaining terms are considered as the second parts, $\boldsymbol{K}_l$ and $\boldsymbol{M}_l$.

$$(K_G - \lambda M_G)\Phi_m = 0 \tag{3}$$

$$K_G = K_{mm} - K_{ms}K_{ss}^{-1}K_{sm} = K_f + K_l \tag{4}$$

$$\begin{aligned} M_G &= M_{mm} + K_{ms}K_{ss}^{-1}M_{ss}K_{ss}^{-1}K_{sm} - K_{ms}K_{ss}^{-1}M_{sm} \\ &\quad - M_{ms}K_{ss}^{-1}M_{sm} \\ &= \mathrm{M}_f + M_l \end{aligned} \tag{5}$$

Let the corresponding parameters mentioned above (Eqs. (3)-(5)) associated with a subsequently damaged stage be signed by asterisks. The counterparts are then written here (Eqs. (6)-(8)).

$$(K_G^* - \lambda^* M_G^*)\Phi_m^* = 0 \tag{6}$$

$$K_G^* = K_f^* + K_l^* \tag{7}$$

$$M_G^* = M_f^* + M_l^* \tag{8}$$

2.2 An updating procedure

After condensation, the square-reduced matrices with the size of *NS* now are considered as the mechanical properties of a beam-like structure comprised of only lateral DOFs. The health of the i^{th} storey (i = 1, 2, …*NS*) of the structure is defined through only one value of elastic modulus, $\alpha_i E$. The values of α_i are expected to vary from 0 to 1, from a completely damaged to a healthy state**,** respectively. Consequently, there are total *NS* unknown variables contained in the reduced stiffness matrix, $\boldsymbol{K}_G$. Once the j^{th} in-situ measured eigenvalues (λ_j^*) and eigenvectors (Φ^*_{mj}) are obtained from any damaged state, Eq. (6) can be activated. According to the commonly used solution in modal analysis, the required number of measured modes is two as the variables are contained in the reduced stiffness matrix. In this study, the first two lowest modes are taken into account.

The solution for *NS* variables is complicated but it can be simplified using some assumptions. The stiffness matrix at the damaged state written in Eq. (7) includes two parts and both of them contain the unknown variables. The second term, $\boldsymbol{K}_l^*$ is approximately set equal to the counterpart in the intact state, $\boldsymbol{K}_l$. The approach is possible due to the insignificant contribution of slave DOFs. For the rotational ones, there is no mass that is assigned for them so they do not affect the modal results after condensation. For the vertical DOFs, the contribution is insignificant compared to the dominant role of the lateral DOFs at the lowest modes. Finally, as explained before, even the other lateral DOFs are not chosen as master ones that may not affect the results after condensation because there is no significant deviation among nodes on the same level. The lateral displacement of the master DOF on each floor adequately stands for the others. For those reasons, the second term, therefore, contributes insignificantly to the condensed stiffness matrices. The change of this part in post-damaged states compared to the intact state is assumed not to be remarkable. As a result, in this study, the second term of the reduced stiffness matrix containing unknown variables is initially assumed to be equal to the second term of the counterpart in the undamaged state, $\boldsymbol{K}_l$ determined in Eq. (4). Using the same argumentation, the second part of the mass matrix at the damaged state, $\boldsymbol{M}_l^*$ is also initially set as the counterpart in the pristine state, $\boldsymbol{M}_l$. Now only the first part in the reduced stiffness and mass matrices still includes unknown variables. To find out *NS* unknown variables, at least *NS* equations are required. The first *NS*-1 equations can be obtained by substituting the first measured eigenvalues ($\boldsymbol{\lambda}_l$) and eigenvectors ($\boldsymbol{\Phi}_l$) into Eq. (6). This is because the first *NS*-1 equations contain all of *NS* unknown variables, α_i. Then the first equation obtained by substituting the second measured mode into Eq. (6) is added to the required number of equations, *NS*. As a result, the *NS* unknown variables can be computed rapidly. The current result gives the first approximate prediction for the damage scenario. More importantly, this first prediction is then enhanced to better predictions using an updating process.

The initial prediction is obtained approximately so that it contains errors because of the aforementioned erratic assumptions. After the currently obtained stiffness matrix for the damaged state, new reduced stiffness and mass matrices can be computed rapidly due to the condensation procedure. Simultaneously, that sets up a new latter part for each matrix. The currently obtained latter parts are to updates the reduced matrices, $\boldsymbol{K}^*_{1G}$ and $\boldsymbol{M}^*_{1G}$ at the first iteration. As a result, a new system consists of NS-required equations that can be obtained in the same manner. The *NS* equation system is updated and rapidly solved. Consequently, an updating procedure can be generally illustrated as in Eqs. (9)-(11) in which the approximation at the t^{th} iteration is computed based on its previous data.

$$(K^*_{G\_t} - \lambda^* M^*_{G\_t})\Phi^*_m = 0 \tag{9}$$

$$K^*_{G\_t} = K^*_f + K^*_{l\_(t-1)} \tag{10}$$

$$M^*_{G\_t} = M^*_f + M^*_{l\_(t-1)} \tag{11}$$

3. Statistical pattern recognition based DI

For the i^{th} storey or element of the desired vector, let consider the fraction between the elastic modulus of undamaged, E_i, and damaged state, E^*_i of the i^{th} element as written in Eq. (12). The i^{th} element is indicated as damage as β_i is higher than 1. Then, the corresponding value of α_i that is the remaining value of its Young's elastic modulus is computed rapidly due to Eq. (13).

$$\beta_i = \frac{E_i}{E_i^*} \tag{12}$$

$$\alpha_i = \frac{1}{\beta_i} * 100 \tag{13}$$

A more robust technique is set up using statistical criteria to indicate damaged elements from the vector. For a given set of modes, the locations of damage are selected on the basis of a rejection of hypotheses in the statistical sense according to Fukunaga (1990) and Gibson and Melsa (1975). Initially, the value β_i (i = 1, 2, 3, …, *NS*) associated with each member is treated as a random variable, β. In other words, the collection of the damage indices, β, represents a sample population (assume that the variables are distributed normally). The normalized indicator, Z_i, is given by Eq. (14) in which $\overline{\beta t}$ and α_t are the mean and standard deviation of the collection, respectively. Next, the members are assigned to the damage class via a statistical-pattern-recognition technique that utilizes hypothesis testing. The null hypothesis (i.e., H_o) is that the structure is not damaged at the i^{th} member. The alternate hypothesis (i.e., H_1) is that the structure is damaged at the i^{th} member. According to the statistical pattern recognition, damage is confirmed with a confidence of 50% as Z_i equal to 0 while the confidence significantly jumps to 84.1% and 97.7% as the value β_i reaches 1 and 2 respectively. If a criterion for damage is chosen, the decision rule as follows: (1) select H_o (i.e., no damage exists at the i^{th} member if Z_i is less than the criterion or (2) select the alternate H_1 if Z_i is larger or equal to the criterion.

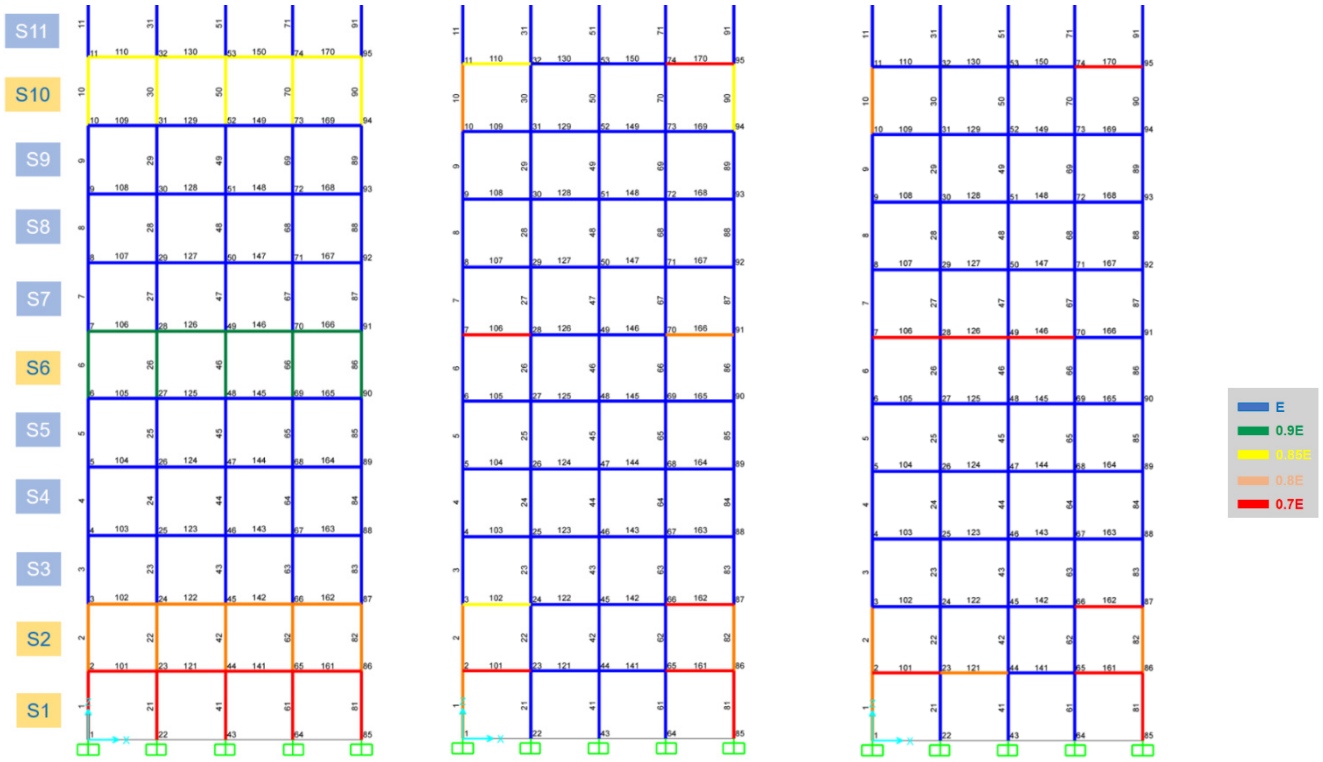

(a) SIM (b) SYM (c) ASY

Fig. 3 Numerical specimen 20S4B

$$Z_i = \frac{\beta_i - \bar{\beta}_t}{\sigma_t} \tag{14}$$

4. Numerical validation for the inverse solution based updating procedure

A numerical validation on the proposed procedure is done on a 20 storey-4 bay building (20S4B) as seen in Fig. 3. The case study is chosen for the purpose of validation and satisfies the behavior of typical high-rise buildings. First, the proposed updating method is built using the inverse solution applied on a simplified model that is obtained using the Guyan condensation technique. Some approximations are made during the simplification. The number of bays is chosen as 4 to force the condensation technique to condense more rotational DOFs to the lateral DOF on each floor. The number of bays of typical high-rise buildings is also around 4. That also has a suitable number of elements or variables that will be considered by the ANN model in the second step. Besides that, choosing a building whose number of stories is lower may increase the lateral stiffness, making its behavior different from typical high-rise buildings. It is worthy that the fundamental period of a high-rise building is approximately equal to the number of stories divided by 10 according to Taranath (2016). The first period of the chosen system is about 1.5 seconds slightly lower than the fraction of 20/10. Therefore, the choice of the numerical specimen is acceptable.

The validation is done in MATLAB®. Steel material with Young's elastic modulus (E) of 210 GPa and the mass density (ρ) of 7850 kg/m^3 are chosen. The constant cross-section of the beam is a rectangle whose dimensions are 40 × 3 mm^2. The equal height of each storey (H) and the equal width of span (B) are 375 mm. It is noted that the section of beams and columns are similar. The thickness is chosen as only 3 mm compared to 40 mm of the width. This is because the contribution of rotational DOFs to the stiffness matrix is assumed to be remarkable to challenge the proposed method built due to the approximation of the Guyan static condensation procedure. The more remarkable contribution of condensed DOFs to the reduced matrices, the more errors are witnessed.

The power of the eigenvalue problem based updating procedure to detect damaged floors is considered from a severe to a light damage scenario as shown in Fig. 3. There are three different models containing different damage scenarios. Only 11 storeys from the base that contains damage are shown with damage scenarios while there is no damage on the other upper floors. As seen in the figure, the blue elements are undamaged and their health is represented by the value of E. Other different colors stand for damages with different severities. In this study, the E value is multiplied by an amount of reduction varying from 0.7 to 1. The first specimen called SIM is the simple case in which all elements of a storey are damaged with the same severity. In the second specimen, called SYM fewer members are damaged on each damaged storey compared to the first model. Damages occur symmetrically on each storey but the severities are different. Finally, the most complicated damage scenario is applied to the model entitled ASY in which damages are located asymmetrically on the frame.

Table 1 Natural frequency

Frame	Mode 1		Mode 2	
	f (Hz)	f* (Hz)	f (Hz)	f* (Hz)
SIM	0.67844	0.65164	2.0407	1.974
SYM		0.66614		2.0135
ASY		0.66524		2.0144

f*: Frequency for damaged states

Table 1 gives information about the frequencies of the two lowest frequencies. It is noted that the upper asterisk sign means the values obtained for damaged cases. Model SIM seems to be damaged most significantly as its frequencies are lower than the counterparts of other models. Specimen SYM owns a higher value for the first frequency and a lower one for the second frequency compared to the counterparts of the specimen ASY. In general, the first two frequencies are similar to the ones of typical high-rise buildings.

The results obtained from the updating procedure are shown in Fig. 4. As seen in the figure, convergence is generally achieved at the 20th iteration for all models. There is some deviation at the first prediction for α values but the parameter for all elements is kept unchanged after converging. The results obtained after the convergences are assumed to be optimum due to the updating procedure.

Presented for consideration in the line graph and bar graphs of Fig. 5, detailing figures for damage indication for monitored buildings using the inverse solution-based technique before (Iteration 0) and after (Iteration 35) activating the updating procedure. The results updated using 35 iterations give the damaged storeys more accurately than the first approximated prediction. The convergence obtained from the updating procedure can be seen in Fig. 4. It is worth noting that the damage criterion is chosen with a confidence level of 50%.

The representative of health for each storey, α, is estimated using the first two modal modes. If the value is less than unity, the damage is theoretically indicated. However, the obtained results are only an approximation because the reduced matrices are obtained by using some assumptions. It is seen that most α values are lower than 1 except in some cases equal to unity as seen in ASY at Iteration 0. On the other hand, the parameter of some upper storeys is higher than 1. Especially, a significant deviation from 1 is witnessed in ASY after updating.

Notwithstanding the complicated observation for each model, for the cases of Iteration 0 and Iteration 35, the change of α value of each storey compared to the general trend of all storeys can become good hints to indicate damage. Particularly, from the base to the top of the buildings, the lines initiates at low values for S1 and S2 with an increasing trend followed by an approximate plattened line (from S3 to S5) that remarkably deeps if the next storey is damaged (only S6 and sometimes also with S7) and a reversal trend to a higher value is witnessed if there is no damage next. After the highest damaged point (S10), the lines gradually decline or increase but there is no more significant dip. It means there is no damage to the remaining points even if their α values are so small. Due to that observation, the highest damaged point can be rapidly indicated, particularly S10. Storeys that are lower than S10

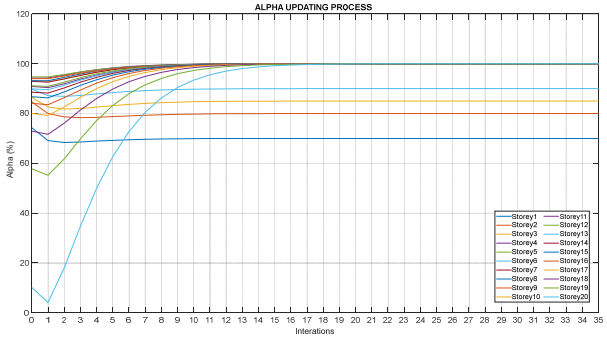

(a) SIM

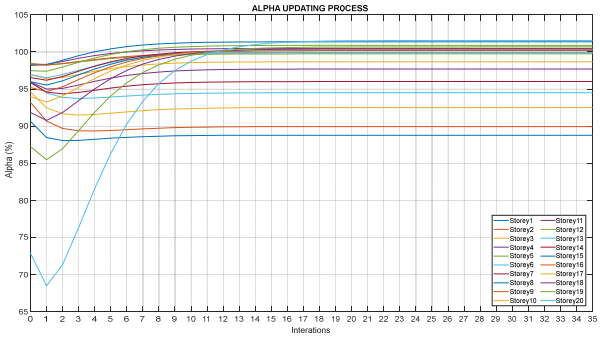

(b) SYM

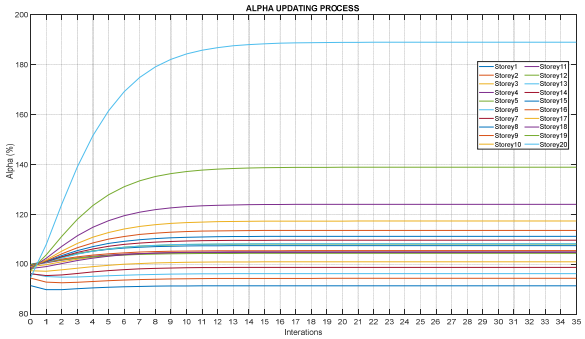

(c) ASY

Fig. 4 Updating procedure

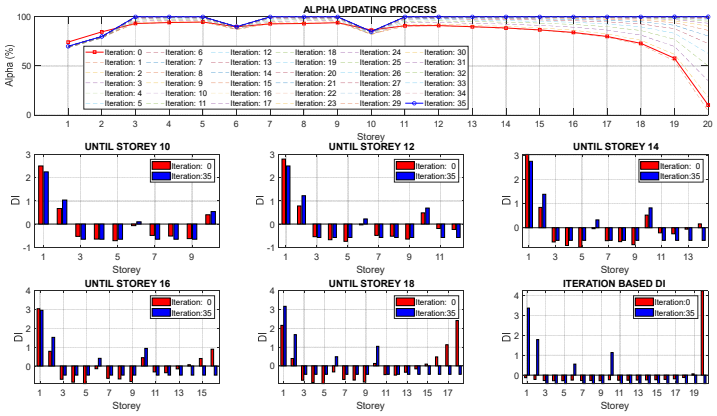

(a) SIM

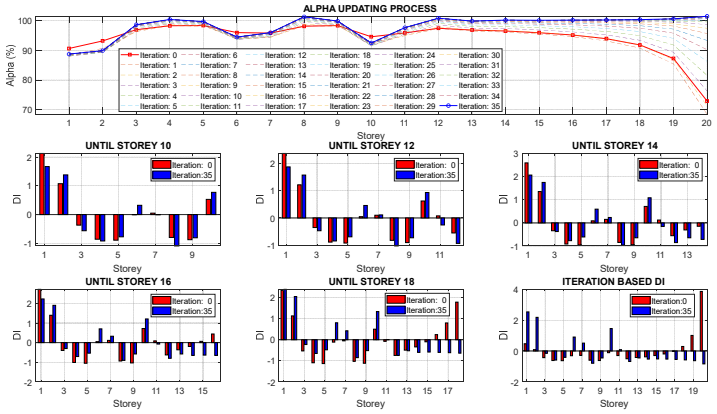

(b) SYM

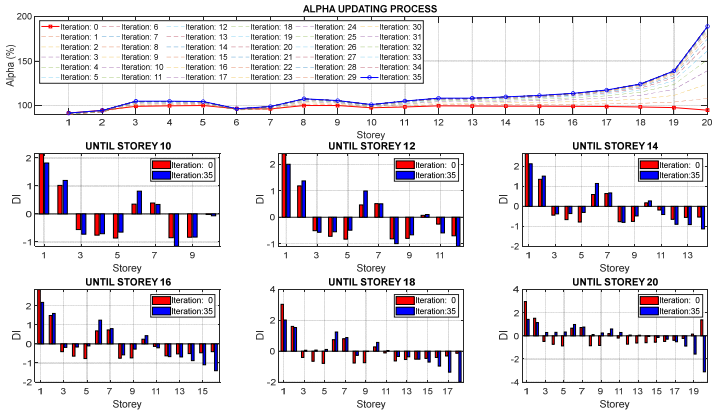

(c) ASY

Fig. 5 Storey-level detection

become potential candidates for damage. Given a list of those candidates, the statistical technique is applied to ensure whether the deeps represent damage or not.

For Iteration 0, as the candidates are limited until S10, the computation then can be considered until S12 due to the aforementioned observation. Among the total four actual damaged storeys, S1 and S2 are always successfully detected with high DI values. S6 and S7 are located in SYM and ASY and while they are completely missed in SIM. Consequently, there are some damages not captured by the first prediction. Therefore, the results should be updated.

One of the more prominent takeaways of the updating procedure is that the updated results are satisfactory enough to detect damaged floors. All of the problems mentioned in the initial prediction are completely overcome for SIM while S7 still appears as a positive false prediction in SYM and ASY. There is no doubt for the precise indication for the SIM because its damage scenario is completely similar to the assumption used as the backbone of the proposed method. In Fig. 5(a), damaged storeys are indicated clearly due to the fact that all of the members on each storey are assigned by the same severity. The line bottoms clearly at damaged points and it is plattened to the unity for undamaged floors. However, as damages do not occur in the

same manner as seen in SIM, the final prediction performs a slight stagnation for SYM and a significant deviation for ASY, especially at the upper storeys. Consequently, even after updated, only the storeys up to S12 are considered for calculating using the statistical technique.

Due to the numerical investigation on the updating approach, it is recommended that before activating the statistical tool the highest damaged point should be predetermined based on the tendency of the lines. After that, one floor after the highest point should be included to give a good prediction for the highest point. For example, in ASY, S10 is missed if only 10 storeys are considered but it is indicated as if S12 is also accounted for. Moreover, it is accepted that if damage occurs only on the beams of a storey, its neighbors possibly appear as damage even after updating. This problem can be fixed in the next step. Generally, the inverse solution based updating procedure is successfully validated regardless of the types of damage categories, eg. severe or light, symmetrical or asymmetrical. As a result, a list of potential candidates for damage is achieved and it is important information before activating the next step using ANN.

5. Application ANN for indicating damaged members

The complicated scenarios on ASY and SYM are considered in this part. Given a list of preliminarily detected storeys (S1, S2, S6, S7, and S10), an ANN model that is a multilayer perceptron type is designed to fulfill the actual damage scenarios in which damaged columns and beams are localized. According to Hagan *et al*. (1995), most practical neural networks have just two or three layers while higher orders are rarely applied. However, multiple hidden layers provide greater flexibility for generalization during the learning process and can remarkably reduce the need for a larger number of neurons according to Shih (1994). The author also suggested that a network can have from two to six layers and a wide range of variations in the number of neurons for each hidden layer. In this study, an ANN architecture with one input layer, one output layer, and two hidden layers is applied as seen in Fig. 6. The ANN is trained using the Levenberg-Marquardt backpropagation algorithm. Mean squared error (*mse*) stands for the performance of the ANN.

The length of input (*NI*) and output (*NF*) vectors are determined by the external problem specifications. Each element on the damaged storeys is assigned as an unknown factor in the output layer of the network. That makes a total of 45 *NF* factors. In other words, the health of the desired element is α_eE (e = 1, 2, 3… *NF*). The values of α_e are expected to fall between 0 and 1. However, they can be out of the range due to the accuracy of prediction. The length of input data (*NI*) is dependent on the information chosen to train the network. In this study, modal data is considered as input data that stands for a response of the desired buildings due to each corresponding damage scenario in the training state**.** Two types of input vectors are considered in this study. The first one, called Type 1 consists of the first three eigenvalues and corresponding mode shapes. As a result, Type 1 contains 66 members. These mode shapes are lateral displacement modes obtained from the same measurement point network in the updating procedure. The second vector, namely Type 2 is a more complicated one, includes three information from each storey, the same lateral displacement as in Type 1, two vertical displacements at the starting point, and the ending point of the storey as seen in Fig. 2(a). The ratio between the two vertical information is added to the input vector in spite of the raw vertical displacements. This information approximately stands for the rotation of the storeys. Consequently, the length of the input vector for Type 2 is 126. It is noted that for two types, each eigenvalue is normalized to the highest one and each mode shape is normalized to the amplitudes measured at the top floor.

Due to the type of input and output data that varies generally in the range from -1 to 1 but it may slightly deviation from the range, the *purelin function* (Fig. 7) is selected as the transfer function in all layers. The function results in an output value (a) equal to the input value (n).

For training the network containing 45 factors, a huge number of combinations is necessary. Even only with 2 levels, undamaged and damaged are considered, a total of 2^{45} combinations should be analyzed. To overcome the problem, the OA method is applied. The array, namely OA.96.48.2.3.pal has been built and published in the library of Sloane (2007). The data is built for the case of 48 factors with the 2 levels. There are 96 runs or combinations, significantly low compared to 2^{45}. The array includes two digits 1 and 0 standing for damaged and undamaged, respectively. Moreover, the strength of the array is 3. For the case of 45 factors, a new array in which 45 out of 48 columns are randomly chosen from the original array and the same number of rows (96) is kept is built for the problem in this study. After that, the Latin hypercube sampling technique integrated with MATLAB® is applied to arrange damage severities into the 1-digits of the currently built array. The α values varying from 0.7 to 1 are divided into a specific number of intervals. For instance, there are 1056 runs for training the network as 10 intervals in the range (11-point division) are considered. 75% of the runs are used for training the network, 15% for validation, and 15 % for testing. The model stops as there is no improvement after continuous six iterations based on the validation data.

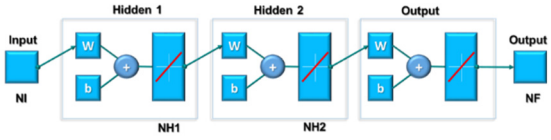

Fig. 6 Proposed ANN architecture

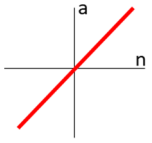

Fig. 7 Purelin transfer function

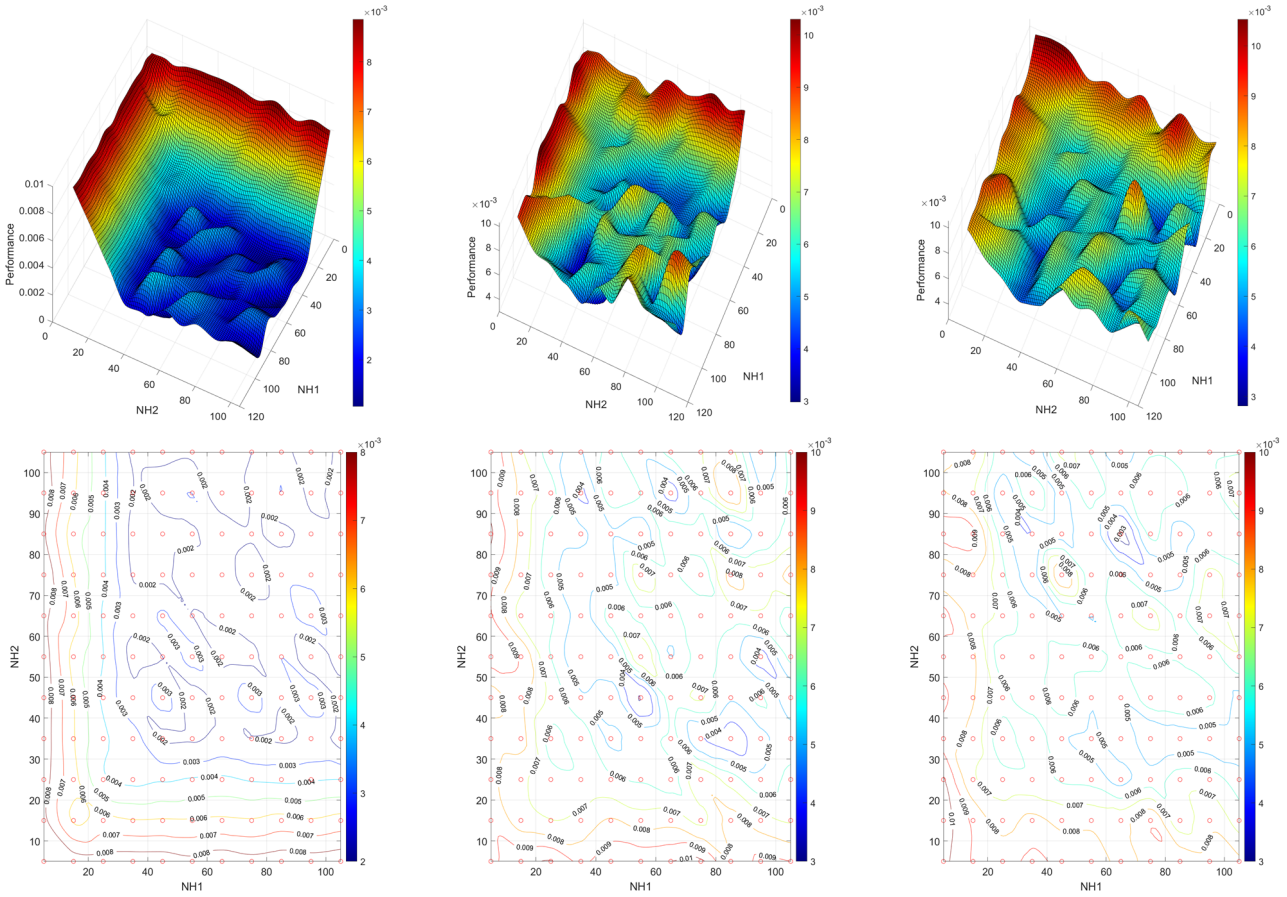

(a) Training (b) Validation (c) Testing

Fig. 8 Performance surfaces

After the completion of training, the trained ANN is decided to be reasonable or not due to some criteria according to Beale *et al*. (2018). First, based on the performance lines, the final *mse* is small. Next, the *mse* value for validation and test data subsets have a similar characteristic. Finally, no significant overfitting issue is captured until the epoch at which the optimal validation occurs. Overfitting is defined for the case in which good performance is achieved after training using the training subset while poor predictions are captured for the validation and test sets. Additionally, Sahin and Shenoi (2003) chose the network based on the minimum *mse* and better convergence with an increase in the number of epochs. In this study, the *mse* value and the performance of training, validation, and test are considered. After that, the correlation between the desired targets and predicted outputs, *R*-value, is also taken into account.

As the size of hidden layers is concerned, there is no standard rule to select an appropriate number of neurons for each hidden layer. The parameter is dependent on the types of problems. Gately (1996) recommended that the number of hidden nodes can be set equal to the total number of inputs and outputs. Bakhary (2008) applied a trial and error method to select the number of neurons for a network with a unique hidden layer. An appropriate number of neurons was indicated based on the lowest performance value. In this study, the network is more complicated, a trial and error method is applied to look for an initial hint to choose the number of neurons for two hidden layers (*NH1* and *NH2*). From the range of α values of 0.7-1, only three intervals (4-point division) is considered for the purpose of speeding up the training process. Type 2 is used to build the input dataset. The values of NH1 and NH2 vary from 5 to 105 with an interval of 10, making 121 combinations resulting in 121 *mse* values. The performance surfaces are picturized in Fig. 8.

Fig. 8 demonstrates the performance surfaces based on the *mse* values obtained by each combination of *NH1* and *NH2*. According to the three-dimensional surfaces and the corresponding contours, it is observed that the combinations of *NH1* and *NH2* that are higher than 35 probably lead to good predictions. First of all, the training performance (Fig. 8(a)) picturizes the valleys containing lower *mse* values. The surface starts from the high amplitudes of about 0.008 as the two parameters are approximately less than 10. A gradual declination is witnessed as they are continuously increased to 30 in which *mse* is captured at a value of 0.003. As the number of neurons continues increasing more than 35, the surfaces seem to bottom at a mse value of around 0.002. Although a unique dip is not indicated clearly at the valley with a slight stagnation, the value of *mse* does not change remarkably. There are some peaks with an amplitude of 0.003 at the valley but the slight deviation is not a case. The predictions herein are obtained using

randomly chosen weight and bias matrices. More repetition may give smoother surfaces. Moreover, it should be remembered that these surfaces are only the approximations that are built as *NH1* and *NH2* are divided with an interval of 10, not a fairly refined division. However, the surfaces are adequate to get a hint for selecting the number of neurons. Additionally, for the validation and test performances (Figs. 8(b)-(c)), approximately similar surfaces are also achieved, even slightly complicated performances at the valley are witnessed. The *mse* values achieved using the validation and test subsets are generally higher than the ones using the training data. For fewer neurons in the hidden layers, from 5 to 20, the *mse* values decline from 0.009 to 0.007. After that, the values gradually decrease but are still higher than the valley values obtained using the training set. The *mse* values at the valley vary from 0.004 up to 0.008. The *mse* of 0.04 and 0.03 are also predicted but they are not predominant in the valleys. However, the validation and test performances show an approximately similar performance. The training part using 70% of the database is assumed to give a better performance with a clear surface whose valley is smoother and more stable. According to the training surface, the number of neurons in the hidden layers higher than 35 may not make a significant change from the *mse* value of 0.002. Additionally, in the training performance, it is observed that as more than 35 neurons in each hidden layer are used, a well-trained network can be achieved regardless of the ratio between *NH1* and *NH2*. As a result, an initial hint can be obtained with the number of *NH1* and *NH2* higher than 35 and the hidden layers can have the same number of neurons. It is decided that 45 neurons are chosen for the two hidden layers. Particularly, an ANN architecture of 126:45:45:45 is built using Type 2 input data. The size of hidden layers can be adjusted based on the performance of training, validation, and test data. Moreover, the correlation coefficient between desired targets and predicted outputs, *R*-value is also considered for adjusting.

The proposed ANN model is applied to figure out the damage scenario of ASY containing a light and asymmetrical damage scenario. A total of 45 α-values of columns and beams are achieved after feeding the Type 2 input set to the trained ANN. The values lower than unity are theoretically determined as damage. However, this is only an approximation, the α value of undamaged elements may be slightly underestimated from unity. Once again, the pattern recognition technique is applied to detect damaged members based on DI values as all 45 members are taken into account. In this step, the damage criterion is set as 0.5, equivalent to the confidence of about 70%. The prediction for the damage scenario on ASY using the trained network is displayed in Figs. 9(a) and 10(a).

Table 2 Performance

Division	Performance			*R*_value
	Training	Validation	Testing	
4-point	0.0022	0.0050	0.0062	0.8539
6-point	0.0014	0.0025	0.0023	0.9185
11-point	0.0014	0.0018	0.0019	0.9216

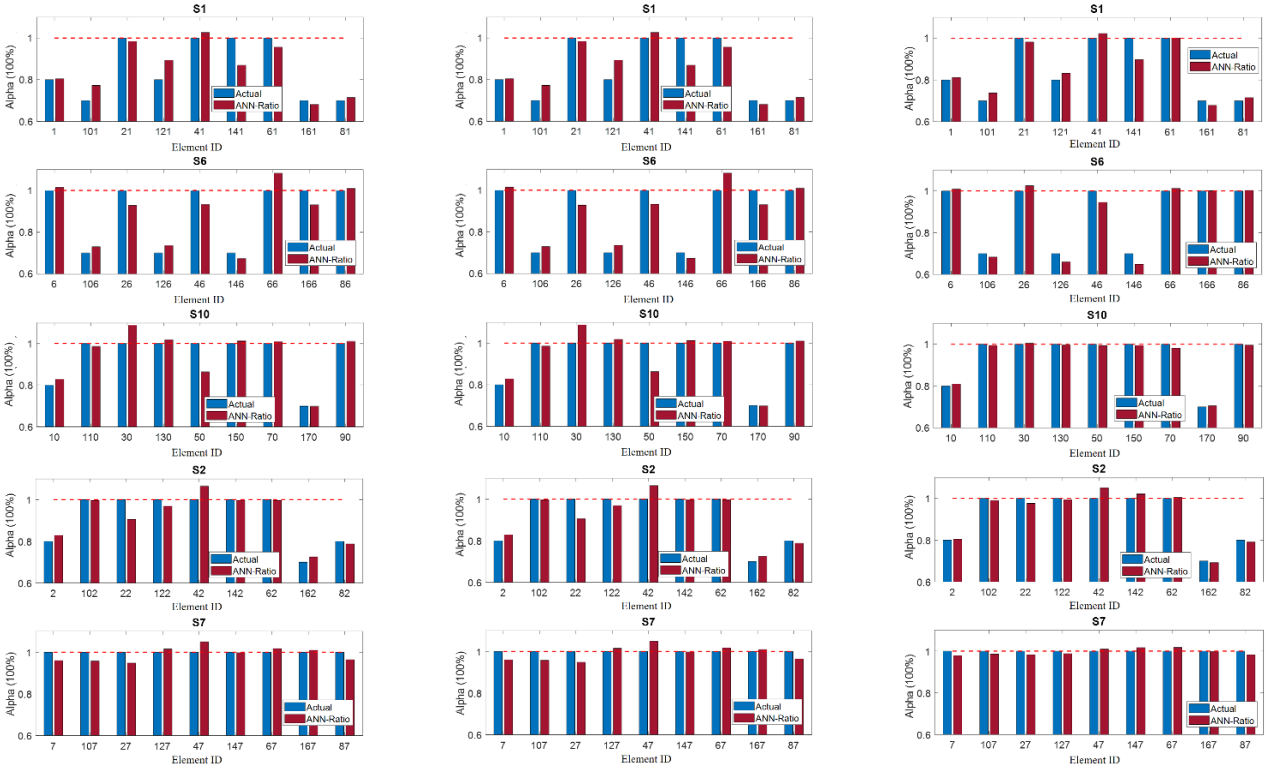

(a) 4-point division (b) 6-point division (c) 11-point division

Fig. 9 ANN-Ratio based α prediction for ASY

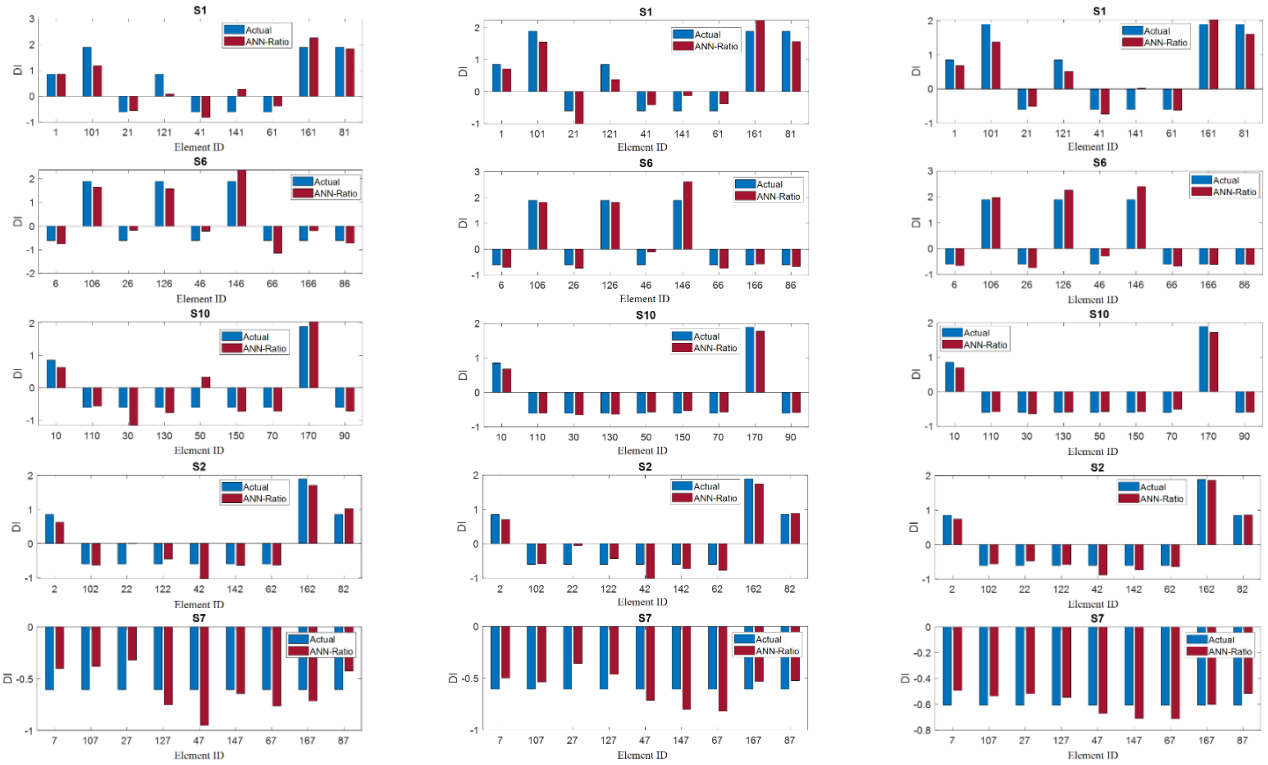

(a) 4-point (b) 6-point (c) 11-point

Fig. 10 ANN-Ratio based DI prediction for ASY

As the input data is built with a three-interval division for the damage range (from 0.7 to 1), the actual damage scenario on ASY is generally detected. First of all, the positive false predicted storey from the previous step, S7 is adjusted to undamaged as the actual case. There is no damage to S7 as predicted by the two network models. The α value of all elements on S7 approximately reaches unity. The corresponding DI values lower than 0 confirm the health of all elements. The damaged components on actual damaged storeys are generally indicated except the false prediction on S1. As the damage criterion is set to 0.5, a negative false is witnessed for element 121, a beam on S1. Moreover, element 141 on S1 and element 50 on S10 have a value of DI slightly less than 0.5 but they possibly reach higher levels if the network is trained again using another randomly chosen weight and bias matrices. This is because the predicted α values for those undamaged elements are remarkably less than unity. Additionally, as seen in Table 2, the *R*-value is only 0.8539. Besides that, the validation performance deviates from the counterpart of test performance, 0.005 compared to 0.0062. The network should be improved for better results. Building more refined data for the input is considered. Higher numbers of intervals, 6 and 11 are then applied to build more refined input data sets. The results are shown in Figs. 9(b)-(c) and Figs. 10(b)-(c).

Figs. 9(b)-(c) and Figs. 10(b)-(c) show the improved damage identification as the damage range is divided with higher resolutions. As the number of intervals increases acceptable predictions can be achieved as the issues left by using the 4-point division. The negative false prediction on component 121 is fixed considering the 11-point division. From the 4-point division, the DI value of this beam gets higher when applying the 6-point division but is still less than 0.5. It reaches the damage criterion as the 11-point division is applied. Moreover, the issue related to component 50 is fixed choosing the 6-point division as its α value is approximately upgraded to the unity. The highest resolution gives the best performance as the *R*-value is up to 0.9216, an acceptable value. Although the final model performs an acceptable prediction with the highest *R*-value, it is still less than the perfect value of unity. There is some slight deviation from the actual values in terms of α values as seen in Fig. 9(c). This is because only a limited number of samples are used to train the network rather than the full set of samples containing numerous cases. With the modest number of combinations, the results certainly deviate around the actual ones but within an acceptable range. For undamaged members as seen in Fig. 9(c), the predicted α values may be higher or lower than unity. However, the differences are really slight and do not affect the accuracy of prediction. This issue cannot be avoided completely using ANN techniques. It can be lessened by increasing the number of investigated combinations. Consequently, it causes a higher cost for computation. It is no need to do that in this situation. The trained network with the *R*-value of 0.9216 obtained in this study is adequate to detect damaged elements. According to Beale *et al*. (2018), the parameter reaching 0.93 gives a good prediction. Moreover, the performances for training, validation, and test subset are also closed to each other. The trained network, therefore, is considered the best one with an acceptable *R*-value and

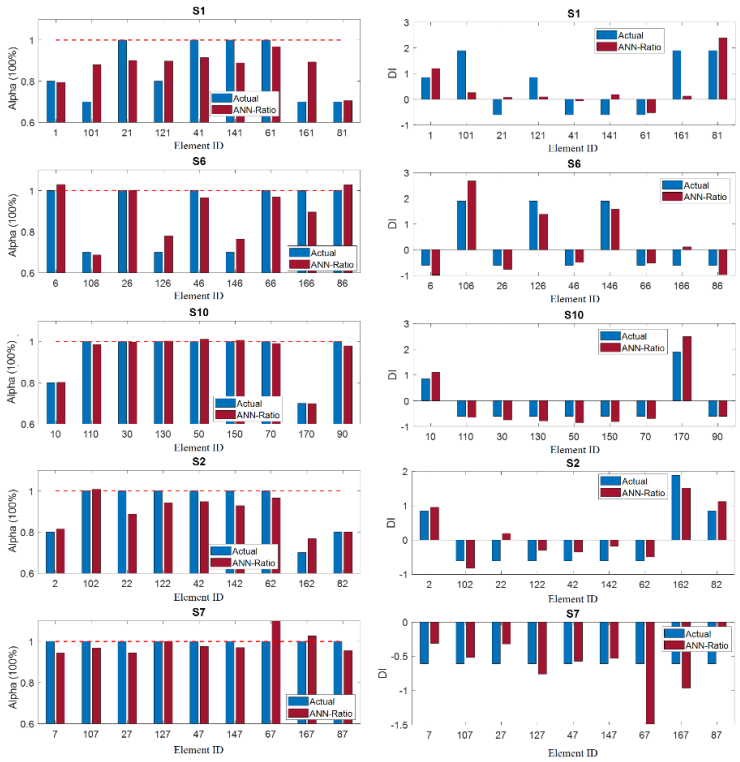

Fig. 11 ANN-Ratio based prediction for ASY using only mode 1

good performance.

To speed up the training process, the size of Type 2 input is reduced by using only the information from mode 1 despite 3 modes, and the results are then shown in Fig. 11. The information using only mode 1 is inadequate to get accurate results. In terms of damage localization, the worst prediction transpires in S1. Particularly, the components 101 and 161 that are two beams cannot be detected. The damaged column, 121 is also missed. That is not acceptable because columns play an important role in high-rise

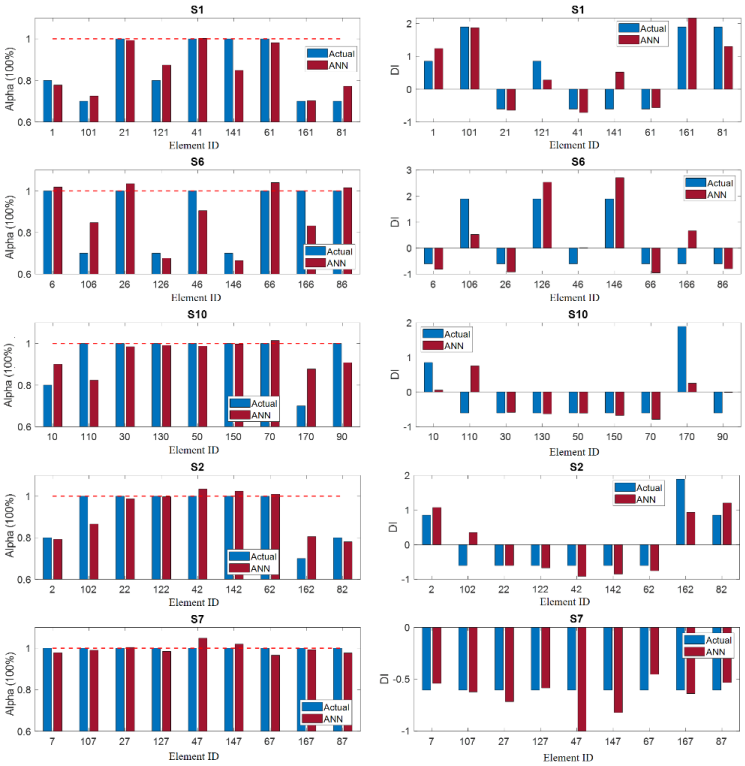

Fig. 12 Damage identification for ASY using Type 1

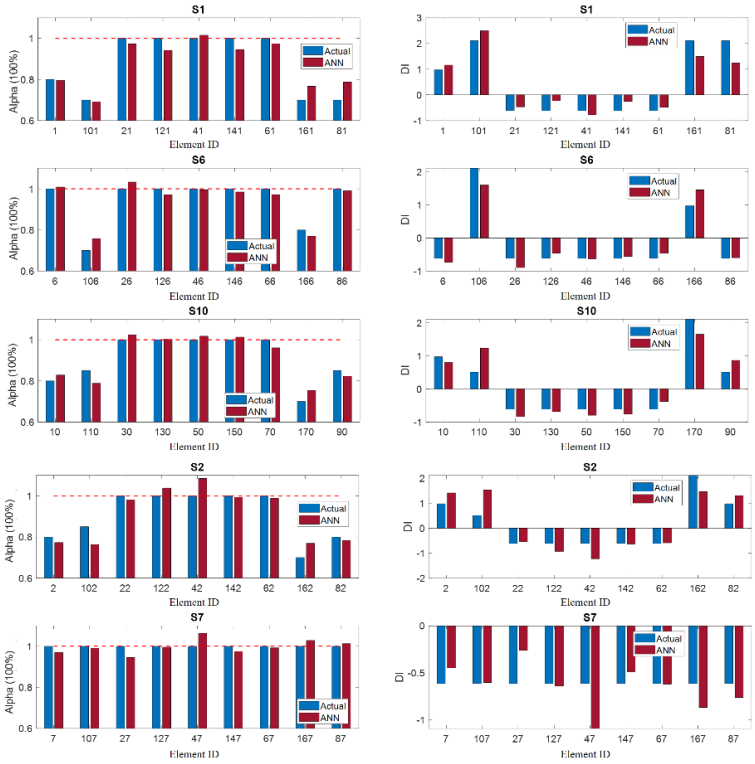

Fig. 13 Damage identification for SYM using Type 1

buildings. The damage detection for other storeys is generally precise. S7 is successfully predicted as undamaged. However, the severity of elements cannot be estimated accurately, especially on S1. It can be claimed that the input data using only the first mode is not enough to train a network.

Presented for investigation in the bar graphs (Fig. 12), detailing results for damage identification at element levels of ASY using the Type 1 input data in which only the lateral displacements are concerned while the information related to the rotation of storeys is ignored. Generally, observe that the ANN trained using Type 1 is not powerful even if it can predict that S7 is not damaged. The network trained using Type 1, namely ANN, seems to give acceptable results for an approximately symmetrical scenario. Moreover, the α value of some elements is estimated inaccurately, especially on S1. That causes positive false predictions for some components such as 141, 166, 110. Additionally, the elements 121, 106, 10, 170 are undetectable as their DI is less than the criterion. All those issues are not witnessed in the case of ANN-Ratio. It can be concluded that Type 1 is inadequate to train the network. This is because using only the lateral displacement information is not capable of distinguishing damage occurring asymmetrically. Contrarily, it possibly leads to acceptable predictions for the case of symmetrical categories like SYM.

Type 1 input data using less information is not powerful enough to predict an asymmetrical damage category but it can lead to good results for a symmetrical damage scenario as seen in Fig. 13. As damage occurs symmetrically on the system such as SYM, all damaged members are accurately indicated regardless of the difference in terms of severity of each symmetrical couple. For instance, on S6, the elements 106 and 166 are damaged with different levels but they are precisely detected using Type 1 data. Moreover, as seen in the case of ASY, S7 is also confirmed herein as a healthy storey. It can be concluded that Type 1 input data using only the information of lateral displacements is robust enough to identify damage on buildings that are mostly damaged symmetrically. If this information can be preliminarily confirmed, using Type 1 input data is suitable for the practical application because further required data such as vertical displacements cause a higher cost for arranging suitable sensor networks. More importantly, the vertical displacements are generally smaller than the lateral ones. Consequently, it is difficult to measure them.

6. Conclusions

Aim at determining a damage scenario on a high-rise building containing a huge number of elements. The outstanding of the technique is overcoming the issues related to an enormous number of DOFs on high-rise buildings using a 2-step approach. Element-level damage detections are obtained successfully using only the first three modes. In general, the required number of measurement points is equal to the number of storeys, making it significantly low compared to the full system of DOFs. One measurement point per floor is adequate to detect damaged storeys. This information can lead to acceptable element-level detections when damage scenarios are symmetrical. That is generally compatible with real conditions. Additionally, for element-level detection on an

asymmetrical scenario, two more vertical DOFs on each floor should be added. However, it is not the case as the number of measured DOFs is still significantly less than the complete number.

The first step is to detect damaged storeys and then the second one indicates damaged components. For the first purpose, a powerful method built based on the eigenvalue problem is proposed. The approach is sufficient discrimination for reliable damage detection at storey levels using only the lowest two modal modes. A state-of-the-art investigation is done on a building containing a light and asymmetrical damage category. For the second step, given a limited number of damaged storeys, an ANN model is applied to indicate damaged elements in these levels. That reduces significantly the number of desired elements for the ANN compared to a model working with a complete number of elements. The network that is designed using the first three modal lateral displacements and the information related to the rotation of the storeys is capable of localizing damage and estimating damage severity. From the numerical investigation on a 20-storey building, there is some notable information that can be written here.

- The eigenvalue problem based methods are powerful to recognize the changes in terms of stiffness between two states of a structure using only the first two lowest modal modes. The approach leads to good results for the case of heavy damage scenarios. Nevertheless, lighter and more complicated damage scenarios cannot lower the robustness of the proposed approach.
- As damage only occurs on beams, positive false predictions may be witnessed on the upper neighbor of the actually damaged floors.
- The ANN model trained using lateral displacement and the information related to the rotation of storeys of the first lowest three modes exactly localizes damaged elements regardless of the complexity of damage scenarios. The damage severity of each element is also estimated with high accuracy.
- The ANN model trained using only the information of lateral modal displacement is not able to predict accurately asymmetrical damage scenarios. False predictions appear and damage severities are obtained with low accuracy. However, for a symmetrical damage category, the network gives good results for damage identification.
- The damage range should be divided as small as possible to improve the performance of ANNs. Through the numerical investigation done in this study, the damage range should be divided using at least 10 intervals to get acceptable predictions based on the *R*-value, the performances of training, validation, and test sets.
- Additionally, the manuscript also contributes a general view when choosing the number of neurons for a network whose number of hidden layers is 2. According to the full trial and error investigation, the number of neurons in the hidden layers can be chosen by the same value.

The proposed two-step procedure is successfully validated using only numerical simulations. However, the technique should be investigated more before applying to real buildings because the modal data is not easy to be obtained accurately in practice. Experimental validations should be done in the future to ensure that the method can give acceptable damage detections when the measured data is noise contaminated. The operational and environmental effects should be considered.

References

ACI Committee Report SP-97 (1985), Response of Buildings to Lateral Forces, American Concrete Institute; Detroit, MI, USA.

Bakhary, N. (2008), "Structural condition monitoring and damage identification with artificial neural network", Ph.D. Dissertation; School of Civil and Resource Engineering, The University of Western Australia, Australia.

Beale, M.H., Hagan, M.T. and Demuth, H.B. (2018), Neural Network Toolbox™ Getting Started Guide, The MathWorks Inc., MA, USA.

Cerri, M.N. and Vestroni, F. (2000), "Detection of damage in beams subjected to diffused cracking", *J. Sound Vib*., **234**(2), 259-276. https://doi.org/10.1006/jsvi.1999.2887

Chang, C.M., Lin, T.K. and Chang, C.W. (2018), "Applications of neural network models for structural health monitoring based on derived modal properties", *Measurement*, **129**, 457-470. https://doi.org/10.1016/j.measurement.2018.07.051

Dinh-Cong, D., Pham-Toan,T., Nguyen-Thai, D. and Nguyen-Thoi, T. (2019), "Structural damage assessment with incomplete and noisy modal data using model reduction technique and LAPO algorithm", *Struct*. *Infrastruct*. *Eng*., **15**(11), 1436-1449. https://doi.org/10.1080/15732479.2019.1624785

Fukunaga, K. (1990), *Introduction to Statistical Pattern Recognition*, Academic Press, New York, USA.

Gately, E. (1996), *Neural Networks for Financial Forecasting*, John Wiley and Sons, New York, USA.

Gibson, J.D. and Melsa, J.L. (1975), *Introduction to Nonparametric Detection with Applications*, Academic Press, New York, USA.

Gillich, G.R., Furdui, H., Abdel-Wahab, M. and Korka, Z.I. (2019), "A robust damage detection method based on multi-modal analysis in variable temperature conditions", *Mech*. *Syst*. *Signal*. *Process*., **115**, 361-379. https://doi.org/10.1016/j.ymssp.2018.05.037

Hamad, W.I., Owen, J.S. and Hussein, M.F.M. (2011), "A flexural crack model for damage detection in reinforced concrete structures", *Proceedings of the 9th International Conference on Damage Assessment of Structures* (*DAMAS 2011*), St Anne's College, University of Oxford, Oxford, UK, July. https://doi.org/10.1088/1742-6596/305/1/012037

Hagan, M.T., Demuth, H.B. and Beale, M. (1995), *Neural Network Design*, PWS Publishing Company.

Hedayat, A.S., Sloane, N.J.A. and Stufken, J. (1999), *Orthogonal Arrays – Theory and Applications*, Springer Verlag, New York, USA.

Helton, J.C. and Davis, F.J. (2003), "Latin hypercube sampling and the propagation of uncertainty in analyses of complex system", *Reliab*. *Eng*. *Syst*. *Safe*., **81**(1), 23-69. https://doi.org/10.1016/S0951-8320(03)00058-9

Khatir, S. and Abdel-Wahab, M. (2018), "Fast simulations for solving fracture mechanics inverse problems using POD-RBF XIGA and Jaya algorithm", *Eng*. *Fract*. *Mech*., **205**, 285-300. https://doi.org/10.1016/j.engfracmech.2018.09.032

Khatir, S., Abdel-Wahab, M., Boutchicha, D. and Khatir, T.

(2019), "Structural health monitoring using modal strain energy damage indicator coupled with teaching-learning-based optimization algorithm and isogoemetric analysis", *J. Sound Vib*., **448**, 230-246. https://doi.org/10.1016/j.jsv.2019.02.017

Khatir, S., Boutchichab, D., Thanh, C.L., Tran-Ngoc, H., Nguyen, T.N. and Abdel-Wahab, M. (2020), "Improved ANN technique combined with Jaya algorithm for crack identification in plates using XIGA and experimental analysis", *Theor. Appl. Fract. Mech*., **107**, 102554. https://doi.org/10.1016/j.tafmec.2020.102554

Kim, J.T. and Stubbs N. (1995a), "Damage detection in offshore jacket structures from limited modal information", *Int. J. Offshore Polar*, **5**(1), 58-66.

Kim, J.T. and Stubbs, N. (1995b), "Model-uncertainty impact and damage-detection accuracy in plate girder", *J. Struct. Eng*., **121**(10), 1409-1417. https://doi.org/10.1061/(ASCE)0733-9445(1995)121:10(1409)

Kim, J.T. and Stubbs, N. (2002), "Improved damage identification method based on modal information", *J. Sound Vib*., **252**(2), 223-238. https://doi.org/10.1006/jsvi.2001.3749

Mirzabeigy, A. (2019), "An inverse approach based on uniform load surface for damage detection in structures", *Smart Struct. Syst*., *Int. J*., **24**(2), 233-242. https://doi.org/10.12989/sss.2019.24.2.233

Ndambi, J.M., Vantomme, J. and Harri, K. (2002), "Damage assessment in reinforced concrete beams using eigenfrequencies and mode shape derivatives", *Eng. Struct*., **24**(4), 501-515. https://doi.org/10.1016/S0141-0296(01)00117-1

Nguyen, T.Q. (2020), "Damage identification for high-rise buildings using an eigen-problem based approach and an artificial neural network", Ph.D. Dissertation Report; Department of Civil Engineering, Bursa Uludağ University, Bursa, Turkey.

Nguyen, H.D., Tran, H., De Roeck, G., Bui, T.T. and Wahab, M.A. (2020), "Damage detection in truss bridges using transmissibility and machine learning algorithm: Application to Nam O bridge", *Smart Struct. Syst*., *Int. J*., **26**(1), 487-499. http://dx.doi.org/10.12989/sss.2020.26.1.035

Paral, A., Roy, D.K.S. and Samanta, A.K. (2019), "Application of a mode shape derivative-based damage index in artificial neural network for structural damage identification in shear frame building", *J. Civil Struct. Health Monitor*., **9**, 411-423. https://doi.org/10.1007/s13349-019-00342-x

Rizos, P.F., Aspragathos, N. and Dimarogonas, A.D. (1990), "Identification of crack location and magnitude in a cantilever beam from the vibration modes", *J. Sound Vib*., **138**(3), 381-388. https://doi.org/10.1016/0022-460X(90)90593-O

Rytter, A. (1993), "Vibration based inspection of civil engineering structures", Dissertation; University of Aalborg, Denmark.

Sahin, M. and Shenoi, R.A. (2003), "Quantification and localisation of damage in beam-like structures by using artificial neural networks with experimental validation", *Eng. Struct*., **25**(14), 1785-1802. https://doi.org/10.1016/j.engstruct.2003.08.001

Shih, Y. (1994), *Neuralyst user's Guide*, Cheshire Engineering Corporation.

Sloane, N.J.A. (2020), *A Library of Orthogonal Arrays*. http://neilsloane.com/oadir/

Smith, S.N. and Coull, A. (1991), *Tall Buildings Structures*: *Analysis and Design*, John Wiley and Sons, NJ, USA.

Taranath, B.S. (2016), *Tall Building Design*: *Steel*, *Concrete*, *and Composite Systems*, CRC Press.

Tran-Ngoc, H., Khatir, S., De Roeck, G., Bui-Tien, T., Nguyen-Ngoc, L. and Abdel-Wahab, M. (2018), "Model updating for Nam O bridge using particle swarm optimization algorithm and genetic algorithm", *Sensors*, **18**(12), 4131. https://doi.org/10.3390/s18124131

Tran-Ngoc, H., Khatir, S., Le_Xuan, T., De Roeck, G., Bui-Tien, T. and Abdel-Wahab, M. (2020), "A novel machine-learning based on the global search techniques using vectorized data for damage detection in structures", *Int. J. Eng. Sci*., **157**, 103376. https://doi.org/10.1016/j.ijengsci.2020.103376

Wahalthantri, B.L., Thambiratnam, D.P., Chan, T.H.T. and Fawzia, S. (2012), "An improved method to detect damage using modal strain energy based damage index", *Adv. Struct. Eng*., **15**(5), 727-742. https://doi.org/10.1260/1369-4332.15.5.727

Yan, Y.J., Cheng, L., Wu, Z.Y. and Yam, L.H. (2007), "Development in vibration-based structural damage detection technique", *Mech. Syst. Signal Pr*., **21**(5), 2198-2211. https://doi.org/10.1016/j.ymssp.2006.10.002

Yun, C.B. and Bahng, E.Y. (2000), "Substructural identification using neural networks", *Comput. Struct*., **77**(1), 41-52. https://doi.org/10.1016/S0045-7949(99)00199-6

Yun, C.B., Yi, J.H. and Bahng, E.Y. (2001), "Joint damage assessment of framed structures using a neural networks technique", *Eng. Struct*., **23**(5), 425-435. https://doi.org/10.1016/S0141-0296(00)00067-5

HJ